

# Structure, Bonding, and Reactivity in Transition-Metal-Inserted Thiophene Complexes

Michael Palmer, Kay Carter,<sup>†</sup> and Suzanne Harris\*

Department of Chemistry, University of Wyoming, Laramie, Wyoming 82071-3838

Received August 19, 1996<sup>⊗</sup>

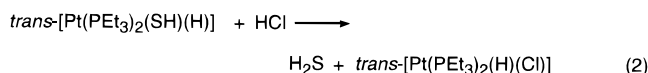
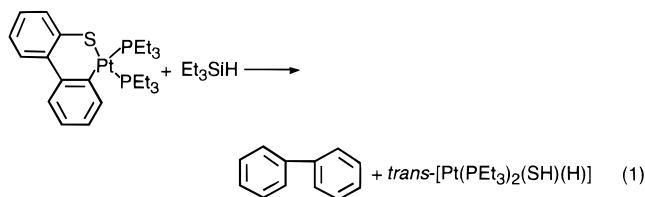
Fenske–Hall molecular orbital calculations are reported for a number of structurally characterized transition-metal-inserted thiophene complexes. These complexes differ from one another in terms of metal center, ligands, coordination number, and metallacycle geometry. The results of the molecular orbital calculations demonstrate that many of these complexes are not only structurally but also electronically similar. Many of the complexes have a HOMO that is predominantly sulfur in character. This suggests a susceptibility toward electrophilic attack at the sulfur similar to that observed in  $(\text{PEt}_3)_2\text{Pt}[C,S-(\text{SC}_{12}\text{H}_8)]$  and  $(\text{triphos})\text{Ir}(\text{H})[C,S-(\text{SC}_8\text{H}_6)]$ . The reactivity of a number of platinum- and (triphos)iridium-inserted complexes toward hydride addition is consistent with the fact that these are the only molecules that have a metal-based LUMO accessible to an attacking nucleophile. A combination of molecular orbital and molecular mechanics calculations suggests that the differences in metallacycle geometry observed in 18-electron complexes, planar and bent, arise primarily from steric rather than electronic factors. The delocalization of the metallacycle bonding which is observed in a few metal-inserted complexes is directly related to electron deficiency in the complexes and the orbital structure associated with specific coordination geometries.

## Introduction

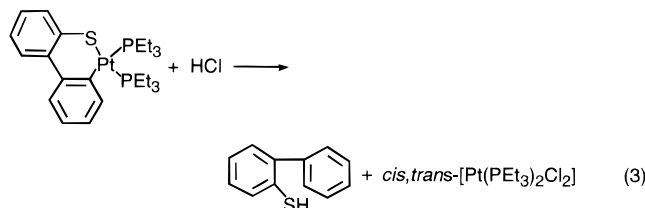
In recent years, there has been considerable interest in investigating the mechanistic details of hydrodesulfurization (HDS) as it relates to thiophene (T) and derivatives such as benzo[*b*]thiophene (BT) and dibenzo[*b,d*]thiophene (DBT). This interest is motivated by the petroleum and coal industries' desire to produce fuels with increasingly lower sulfur contents. Presently, most residual sulfur stems from unsuccessful attempts to remove thiophene and its derivatives from sulfur-laden feedstocks.<sup>1</sup> Successful removal of these thiophenic forms is dependent on a better and more thorough understanding of HDS.

One area of specific mechanistic interest involves the mode by which thiophene and its derivatives might bind to the metal sulfide surfaces used in the HDS process. Studying the high-pressure, high-temperature, heterogeneous catalytic processes involved in desulfurization, however, is intrinsically difficult, and consequently many researchers have prepared and characterized homogeneous transition-metal-based HDS models. These model complexes illustrate numerous metal-thiophene binding modes.<sup>2,3</sup> One of these, a ring-opened or metal-inserted mode, results from the insertion of a transition metal into a C–S bond of thiophene or a derivative. Some of these metal-inserted compounds have demonstrated chemistry which leads to sulfur removal from the thiophenic moiety. For example, Maitlis and Garcia have reported the insertion of Pt(0) into the C–S bond of T, BT, and DBT to form square-planar thiaplattina-

cycles. The T, BT, and DBT complexes can be cleaved, to varying degrees, with several hydridic reagents to yield C<sub>4</sub> hydrocarbons, styrene, and biphenyl, respectively (eqs 1 and 2). In addition, protonation of the



platinum-inserted dibenzothiophene complex results in 2-phenylthiophenol via acid cleavage of the Pt–C and the Pt–S bonds (eq 3).<sup>4,5</sup> Bianchini and Sánchez-



Delgado have also reported desulfurization of the iridium-inserted benzothiophene complex  $(\text{triphos})\text{Ir}[C,S-(\text{SC}_8\text{H}_6)]^+$  (triphos =  $\text{CH}_3\text{C}(\text{CH}_2\text{PPh}_2)_3$ ), via initial hydridic attack at the metal, producing  $[(\text{triphos})\text{Ir}(\text{H})_2\{o\text{-S}-(\text{C}_6\text{H}_4)\text{C}_2\text{H}_5\}]$  (eq 4). The 2-ethylbenzenethiolate ligand

<sup>†</sup>Current address: Department of Chemistry, University of Wisconsin–Parkside, Kenosha, WI 53141-2000.

⊗ Abstract published in *Advance ACS Abstracts*, May 1, 1997.

(1) Topsøe, T.; Clausen, B. S.; Massoth, F. E. *Hydrotreating Catalysis*; Springer-Verlag: Berlin, 1996.

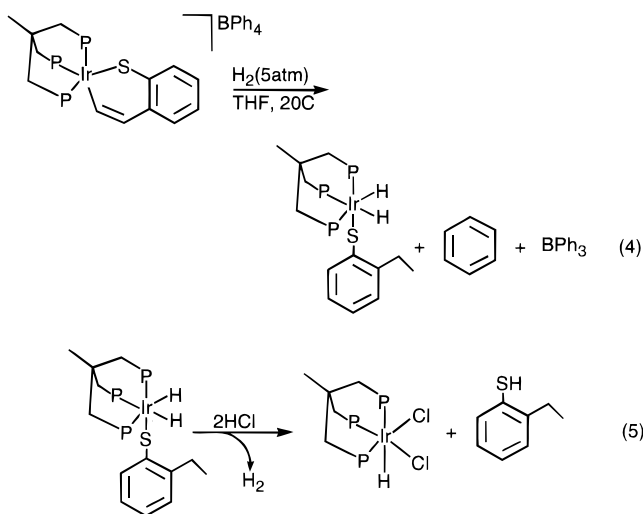
(2) Rauchfuss, T. B. *Prog. Inorg. Chem.* **1991**, *39*, 251.

(3) Angelici, R. J. *Coord. Chem. Rev.* **1990**, *105*, 61.

(4) Garcia, J. J.; Maitlis, P. M. *J. Am. Chem. Soc.* **1993**, *115*, 12200.

(5) Garcia, J. J.; Mann, B. E.; Adams, H.; Bailey, N. A.; Maitlis, P. M. *J. Am. Chem. Soc.* **1995**, *117*, 2179.

can be removed by protonation with HCl (eq 5).<sup>6,7</sup> This

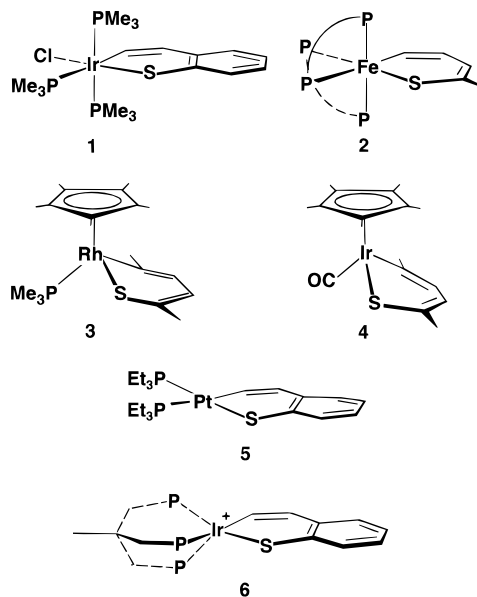


behavior toward sequential  $\text{H}^-$  and electrophile addition was encouraging to Bianchini and co-workers (in terms of modeling heterogeneous HDS chemistry) because of the readily available hydride and proton sources supposedly present on traditional catalytic HDS surfaces.<sup>8</sup> Using the monohydride DBT analog (triphos)IrH(*C,S*-DBT), Bianchini and co-workers have also demonstrated catalytic HDS in the homogeneous phase to produce biphenyl, 2-phenylthiophenol, and  $\text{H}_2\text{S}$  (the same principal products observed in heterogeneous HDS of DBT).<sup>9</sup>

Although these specific platinum- and iridium-inserted complexes exhibit the ability to desulfurize thiophenic molecules, many similar transition-metal-inserted thiophene complexes have not shown such potential as HDS models. This is somewhat surprising, given the similarities of these complexes (Chart 1). Specifically, these complexes are generally formed from late transition metals and incorporate ligands that are principally donor in nature. The differences in reactivity among very similar complexes prompted us to examine the electronic structures of a number of these complexes and attempt to relate the electronic structures to the known reactivities of the complexes. The results of this investigation are reported in this paper.

The first section of this report provides a description of the calculational details. The second section focuses on detailed discussions of the electronic structures, obtained through Fenske–Hall molecular orbital calculations,<sup>10</sup> of six different transition-metal-inserted thiophene and benzothiophene complexes. The complexes differ by one or more distinctive characteristics, including transition metal, coordination number, ligand sphere, and metallacycle geometry (Chart 1). The first two complexes discussed,  $\text{Cl}(\text{PMe}_3)_3\text{Ir}[C,S-(\text{SC}_8\text{H}_6)]$ <sup>11</sup> (**1**) and  $(\text{dmpe})_2\text{Fe}[C,S-2\text{-Me}(\text{SC}_4\text{H}_3)]$ <sup>12</sup> (dmpe = 1,2-bis(dimethylphosphino)ethane) (**2**), are pseudooctahedral

Chart 1



and contain four donor ligands in addition to the thiophene moiety. The near- $C_s$  symmetry of  $\text{Cl}(\text{PMe}_3)_3\text{Ir}[C,S-(\text{SC}_8\text{H}_6)]$  makes the bonding in this compound clear and provides a starting point for a detailed examination of the electronic structure of the complexes. The iron-inserted complex provides insight into effects that a smaller first-row transition metal has on the bonding. The discussion of these complexes is followed by bonding descriptions of two other pseudooctahedral complexes,  $\text{Cp}^*(\text{PMe}_3)\text{Rh}[C,S-2,5\text{-Me}_2(\text{SC}_4\text{H}_2)]$ <sup>13</sup> ( $\text{Cp}^* = \eta^5\text{-pentamethylcyclopentadienyl}$ ) (**3**) and  $\text{Cp}^*(\text{CO})\text{Ir}[C,S-2,5\text{-Me}_2(\text{SC}_4\text{H}_2)]$  (**4**).<sup>14,15</sup> Since these two molecules are structurally analogous, the effects on the electronic structure caused by a  $\sigma$ -donor ( $\text{PMe}_3$ ) versus a  $\pi$ -acceptor ligand (CO) are examined. The last two complexes to be discussed are  $(\text{PEt}_3)_2\text{Pt}[C,S-(\text{SC}_8\text{H}_6)]$ <sup>5</sup> (**5**) and  $(\text{triphos})\text{Ir}[C,S-(\text{SC}_8\text{H}_6)]^{+6}$  (**6**). The bonding in these two complexes is analyzed in terms of their coordination geometries (four-coordinate square-planar and five-coordinate, respectively) and the fact that both of these complexes are reactive toward thiophene degradation.

Although a majority of the metal-inserted thiophene complexes are structurally quite similar, the heterocycles take one of two distinct geometrical conformations. Complexes containing both planar and bent metallacycles have been observed, and the next section of the paper discusses these two different metallacycle geometries. Molecular orbital calculations were used to probe for possible electronic preferences for a particular metallacycle conformation. The results of these calculations suggested that bent-ring geometries do not result from inherent electronic properties. This observation prompted an investigation, using molecular mechanics calculations, into possible steric factors responsible for the bent-metallacycle-ring geometries. Results of molecular mechanics calculations on  $\text{Cp}^*(\text{PMe}_3)\text{Rh}[C,S-2,5\text{-Me}_2(\text{SC}_4\text{H}_2)]$  are discussed. (The investigations into the electronic and steric factors which

(6) Bianchini, C.; Meli, A.; Peruzzini, M.; Vizza, F.; Frediani, P.; Herrera, V.; Sánchez-Delgado, R. A. *J. Am. Chem. Soc.* **1993**, *115*, 7505.

(7) Bianchini, C.; Meli, A.; Peruzzini, M.; Vizza, F.; Moneti, S.; Herrera, V.; Sánchez-Delgado, R. A. *J. Am. Chem. Soc.* **1994**, *116*, 4370.

(8) Bianchini, C.; Meli, A.; Peruzzini, M.; Vizza, F.; Frediani, P.; Herrera, V.; Sánchez-Delgado, R. A. *J. Am. Chem. Soc.* **1993**, *115*, 2731.

(9) Bianchini, C.; Jimenez, M. V.; Meli, A.; Moneti, S.; Vizza, F.; Herrera, V.; Sánchez-Delgado, R. *Organometallics* **1995**, *14*, 2342.

(10) Hall, M. B.; Fenske, R. F. *Inorg. Chem.* **1972**, *11*, 768.

(11) Selnau, H. E.; Merola, J. S. *Organometallics* **1993**, *12*, 1583.

(12) Buys, I. E.; Field, L. D.; Hambly, T. W.; McQueen, A. E. D. *J. Chem. Soc., Chem. Commun.* **1994**, 557.

(13) Jones, W. D.; Dong, L. *J. Am. Chem. Soc.* **1991**, *113*, 559.

(14) Chen, J.; Daniels, L. M.; Angelici, R. J. *Polyhedron* **1990**, *9*, 1883.

(15) Chen, J.; Daniels, L. M.; Angelici, R. J. *Acta Crystallogr.* **1992**, *C48*, 2120.

influence metallacycle geometries are considered in greater detail in a separate publication.)

Finally, the last section of the paper focuses on the reactivity of these complexes. The known reactivities of the platinum and (triphos)iridium complexes are discussed and evaluated in terms of their calculated electronic structures. Possible reactivity of the other complexes is considered in light of similarities in bonding among all the complexes. The effects of different transition metals, ligand spheres, coordination numbers, and metallacycle geometries on the reactivity of these complexes are also discussed.

### Computational Details

**Molecular Orbital Calculations.** All of the results described here were obtained from Fenske–Hall molecular orbital calculations.<sup>10</sup> Orbital populations, overlap populations, and atomic charges were determined with Mulliken population analyses.<sup>16</sup> Bond orders were calculated using the method described by Sannigrahi<sup>17</sup> (this method will be discussed in a future paper).<sup>18</sup>

The 1s through *nd* functions for Fe, Rh, Ir, and Pt were generated by a best fit to Herman–Skillman atomic calculations<sup>19</sup> using the method of Bursten, Jensen, and Fenske.<sup>20</sup> The (*n* + 1)s and (*n* + 1)p functions were chosen to have exponents of 2.0 for Fe, 2.2 for Rh, and 2.4 for Ir and Pt. The carbon and sulfur functions were taken from the double- $\zeta$  functions of Clementi.<sup>21</sup> The valence p functions were retained as the double- $\zeta$  functions, while all the other functions were reduced to single- $\zeta$  functions. An exponent of 1.2 was used for hydrogen.

The molecular structures of all of the transition-metal-inserted thiophene complexes discussed have been determined by X-ray diffraction. These known structures were used for the molecular orbital calculations.

**Molecular Mechanics Calculations.** The results of the molecular mechanics calculations were obtained using the 1.01 Universal Force Field<sup>22–24</sup> as implemented through Cerius<sup>25</sup>. For the calculations on Cp\*(PMe<sub>3</sub>)Rh[C,S-2,5-Me<sub>2</sub>(SC<sub>4</sub>H<sub>2</sub>)], the known, experimental structure for the complex was used as the starting point. To simplify the calculation, the entire molecule, except for the metallacycle, was frozen in space so that movement upon minimization was limited to the thiophene ring system. Pure steric interactions between the metallacycle and the rest of the molecule were desired so as to determine conformational preferences of the ring system based solely on spatial arguments; i.e., minimization should result in the metallacycle being positioned at maximal distances from other substituents. To achieve this, only the following energy terms were employed: bond stretching, torsion, inversion, van Der Waals. Other properties of the molecule, for example the  $\pi$  system in the metallacycle, were simulated through atom typing; i.e. by typing the ring carbon as C\_2, twisting about the C–C bonds was restricted. The other atoms were typed, in accordance with the force field, as follows: rhodium, Rh6+3; sulfur, S\_2; phosphorus, P\_3; thiophene carbon, C\_2; alkyl carbon, C\_3; hydrogen, H\_.

Ligand substitutions were made to determine steric influences on the geometry of the metallacycles. For example, the phosphine group in Cp\*(PMe<sub>3</sub>)Rh[C,S-2,5-Me<sub>2</sub>(SC<sub>4</sub>H<sub>2</sub>)] was replaced with a hydrogen atom in order to identify the effect that a large ligand in that spatial position had on the ring geometry. When ligands were substituted in this manner, the new, smaller ligand was placed coincident with the original ligand at an appropriate bond distance.

### Results and Discussion

The bonding mode of thiophene prior to insertion of a transition metal into a C–S bond has been investigated experimentally. For example, kinetic studies have demonstrated that for Cp\*(PMe<sub>3</sub>)Rh[C,S-2,5-Me<sub>2</sub>(SC<sub>4</sub>H<sub>2</sub>)] an S-bound thiophene species is the immediate precursor to C–S bond cleavage.<sup>26</sup> Because of similarities in the complexes, it is reasonable to suggest that other metal-inserted compounds also form via a similar intermediate, and, in fact, Bianchini and co-workers have substantiated this finding for a number of related complexes.<sup>9,27,28</sup> While the mechanism for ring opening and concomitant metal insertion from an S-bound intermediate is not fully understood, the result is concerted C–S bond cleavage and M–S and M–C bond formation. In this light, it is convenient to view the bonding in these complexes in terms of the interactions between a metal fragment and an “opened” thiophene fragment.

**“Opened” Thiophene Molecular Orbitals.** Similarities in the frontier orbital structures of “ring-opened” thiophene and benzothiophene ligands are apparent (for illustrative examples, see Figures 1 and 2). The HOMO (highest occupied molecular orbital) in these opened fragments is a  $\pi$  orbital perpendicular to the plane of the ring system. A distinctive characteristic of the HOMO is the large percentage of the orbital, 50–65%, centered on the sulfur. The HOMO of the thiophene fragment also contains  $\pi$  electron density on the  $\alpha$ -carbon; the benzothiophene analog contains little  $\alpha$ -carbon character. (Henceforth, the  $\alpha$ -carbon is defined as the carbon on the thiophene moiety which is  $\alpha$  to the metal after insertion.) The SHOMO (second highest occupied molecular orbital) and the LUMO (lowest unoccupied molecular orbital) in the ring-opened fragments are both  $\sigma$  orbitals containing electron density on both the sulfur and  $\alpha$ -carbon. The SHOMO is bonding with respect to the C–S interaction, while the LUMO is antibonding. The separation of the sulfur and  $\alpha$ -carbon produced by opening the thiophene ring system destabilizes the  $\sigma$ -bonding SHOMO and the stabilizes the  $\sigma$ -antibonding LUMO. Consequently, these two orbitals lie relatively close in energy to the fragment's HOMO. The third highest energy occupied and the second lowest unoccupied molecular orbitals are both  $\pi$  orbitals perpendicular to the ring systems. For the thiophene fragments, equivalent electron density resides on both the sulfur and the  $\alpha$ -carbon in these two orbitals. For the opened benzothiophene fragments, the electron density on both of these  $\pi$  orbitals is localized on the  $\alpha$ -carbon. Since the metal-inserted complexes exhibit different

(16) Mulliken, R. S. *J. Chem. Phys.* **1955**, *23*, 1833.

(17) Sannigrahi, A. B. *J. Chem. Educ.* **1988**, *65*, 674.

(18) Lantz, B.; Harris, S. Manuscript in preparation.

(19) Herman, F.; Skillman, S. *Atomic Structure Calculations*; Prentice-Hall: Englewood Cliffs, NJ, 1963.

(20) Bursten, B. E.; Jensen, J. R.; Fenske, R. F. *J. Chem. Phys.* **1978**, *68*, 3320.

(21) Clementi, E. *J. Chem. Phys.* **1964**, *40*, 1944.

(22) Casewit, C. J.; Rappe, A. K.; Colwell, K. S. *J. Am. Chem. Soc.* **1992**, *114*, 10035.

(23) Casewit, C. J.; Rappe, A. K.; Colwell, K. S.; Goddard, W. A., III; Skiff, W. M. *J. Am. Chem. Soc.* **1992**, *114*, 10024.

(24) Casewit, C. J.; Rappe, A. K.; Colwell, K. S. *J. Am. Chem. Soc.* **1992**, *114*, 10046.

(25) Cerius<sup>2</sup>; Version 1.6; Molecular Simulations Inc., 1995.

(26) Dong, L.; Duckett, S. B.; Ohman, K. F.; Jones, W. D. *J. Am. Chem. Soc.* **1992**, *114*, 151.

(27) Bianchini, C.; Herrera, V.; Jimenez, M. V.; Meli, A.; Sánchez-Delgado, R. A.; Vizza, F. *J. Am. Chem. Soc.* **1995**, *117*, 8567.

(28) Bianchini, C.; Jimenez, M. V.; Meli, A.; Vizza, F. *Organometallics* **1995**, *14*, 3196.

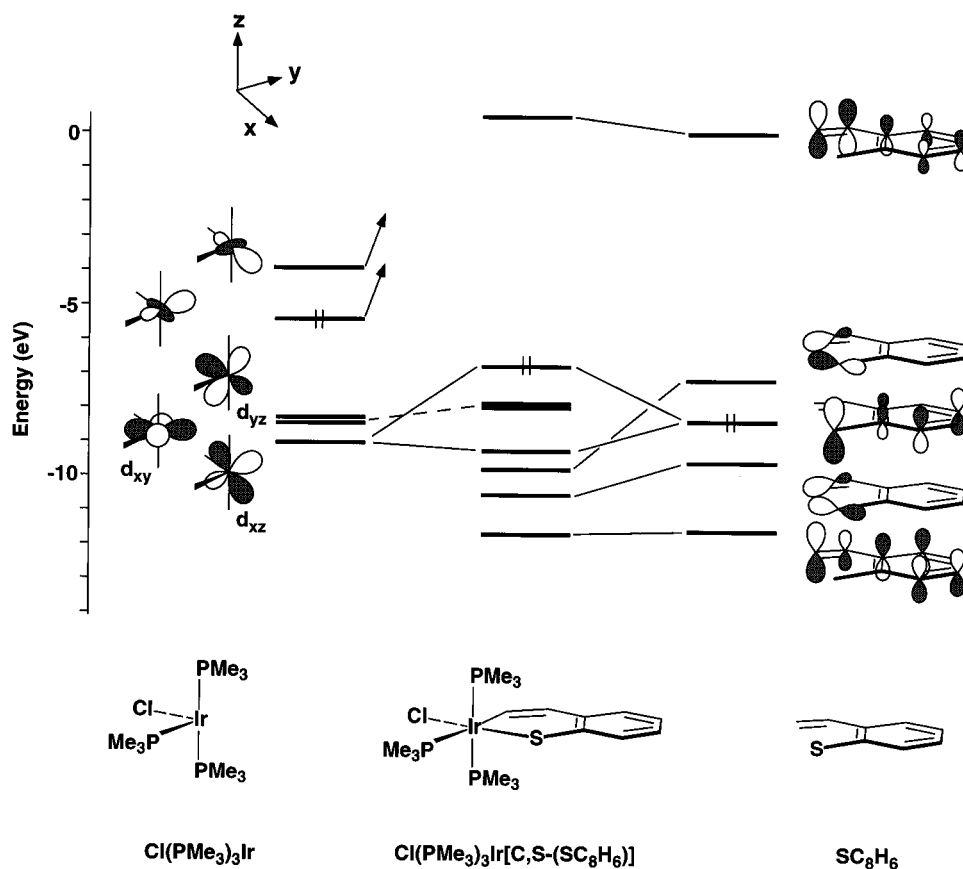


**Figure 1.** Calculated energy level diagrams for  $\text{Cl}(\text{PMe}_3)_3\text{Ir}[C,S-(\text{SC}_8\text{H}_6)]$  and for the  $\text{Cl}(\text{PMe}_3)_3\text{Ir}$  and opened benzothiophene fragments.

coordination numbers and ligand types, the interactions between the opened thiophene fragments and the metal orbitals will be discussed for each specific complex.

**$\text{Cl}(\text{PMe}_3)_3\text{Ir}[C,S-(\text{SC}_8\text{H}_6)]$ .** The molecular orbital interaction diagram for  $\text{Cl}(\text{PMe}_3)_3\text{Ir}[C,S-(\text{SC}_8\text{H}_6)]$  is shown in Figure 1. The bonding interactions between the metal and the benzothiophene are viewed in terms of a  $\text{Cl}(\text{PMe}_3)_3\text{Ir}$  fragment and an opened benzothiophene fragment. These are shown on the left- and right-hand sides of Figure 1, respectively. The " $C_s$ " symmetry of  $\text{Cl}(\text{PMe}_3)_3\text{Ir}[C,S-(\text{SC}_8\text{H}_6)]$  restricts, for the most part, mixing of the  $\sigma$  and  $\pi$  orbitals, and the origins of the interactions between each of the fragment molecular orbitals are clear and distinct. The energy level diagram, consequently, is fairly straightforward.

The metal fragment orbitals are derived from the classic octahedral  $t_{2g}$  and  $e_g$  sets. The  $e_g$  set, however, now consists of two  $\sigma$ -like orbitals formed from combinations of the  $d_z^2$  and the  $d_{x^2-y^2}$  orbitals. One of these metal  $\sigma$  orbitals, the HOMO in the metal fragment, is directed at the incoming  $\alpha$ -carbon, and the other, the LUMO in the fragment, is directed at the incoming sulfur. Both the SHOMO and the LUMO of the benzothiophene fragment ( $\sigma$  orbitals directed at the iridium) have appropriate energies and orientations to interact with the iridium HOMO and LUMO. In this light, the SHOMO can be viewed as donating electron density from the benzothiophene ligand into the LUMO of the metal, while the benzothiophene LUMO accepts electron density from the metal. Overall, the bonding interactions between the metal HOMO and LUMO and the benzothiophene SHOMO and LUMO can be viewed as a formal oxidative addition of the metal, oxidizing Ir(I)

to Ir(III) and forming  $\sigma$  bonds between the iridium center and the sulfur and  $\alpha$ -carbon of the benzothiophene fragment. A formal net transfer of two electrons from the metal to the benzothiophene ligand is evidenced by the fact that the electrons which occupied the HOMO of the metal fragment now reside in metal–ligand bonding orbitals which are primarily localized on the ligand. This transfer of electrons is also reflected in the less negative charge of the iridium in the complex ( $-0.48$ ) compared to that of the iridium in the fragment ( $-0.84$ ).

The metal  $d_{yz}$  and  $d_{xy}$  orbitals are essentially non-bonding in the complex. The filled  $d_{xz}$ , on the other hand, interacts strongly with the HOMO of the opened benzothiophene. This interaction results in a filled bonding/antibonding set of orbitals, and it is the antibonding molecular orbital of the set which forms the HOMO in the complex. The HOMO is notable in that it is primarily ligand-based and, furthermore, predominantly sulfur in character. The HOMO is essentially a lone pair of  $\pi$  electrons isolated on the sulfur. As will be apparent in the later discussion, this filled–filled interaction which results in an antibonding, sulfur-based HOMO in the complex is characteristic of a number of the metal-inserted complexes. The LUMO of the complex is also ligand-based (96%) and is derived almost completely from the second lowest unoccupied orbital of the opened benzothiophene, a  $\pi^*$  orbital. Much of the electron density of this orbital resides on the  $\alpha$ -carbon.

**$(\text{dmpe})_2\text{Fe}[C,S-2\text{-Me}(\text{SC}_4\text{H}_3)]$ .** Because of structural similarities with the iridium-inserted complex, the orbital structure of  $(\text{dmpe})_2\text{Fe}[C,S-2\text{-Me}(\text{SC}_4\text{H}_3)]$  is ex-

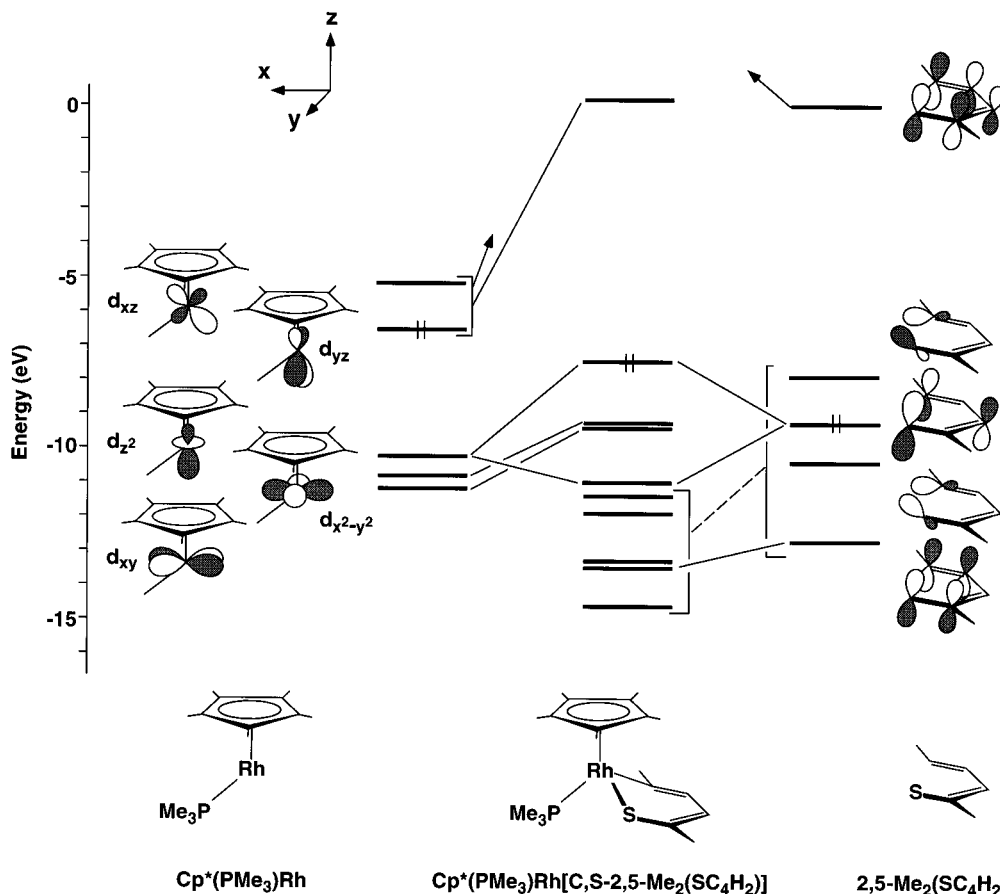


**Figure 2.** Calculated energy level diagrams for  $\text{Cp}^*(\text{PMe}_3)\text{Rh}[\text{C},\text{S}-2,5\text{-Me}_2(\text{SC}_4\text{H}_2)]$  and for the  $\text{Cp}^*(\text{PMe}_3)\text{Rh}$  and  $2,5\text{-Me}_2(\text{SC}_4\text{H}_2)$  fragments.

pected to be similar. (Because of the similarities, no orbital diagram is shown.) Indeed, the thiophene fragment orbitals are comparable in appearance and energy to the benzothiophene fragment orbitals of Merola's iridium complex; the  $(\text{dmpe})_2\text{Fe}$  metal orbitals are comparable in appearance but differ greatly in energy from the  $\text{Cl}(\text{PMe}_3)_3\text{Ir}$  metal orbitals. This difference in energy stems from two factors. First, the charge of the iron in  $(\text{dmpe})_2\text{Fe}$  ( $-1.11$ ) is more negative than the charge on iridium in  $\text{Cl}(\text{PMe}_3)_3\text{Ir}$  due to the additional phosphine donor on the iron complex. Second, the 3d orbitals of iron are inherently higher in energy than the 5d iridium orbitals. These two factors taken together result in the iron orbitals being pushed up approximately 5 eV in energy relative to those of iridium. Consequently, for  $(\text{dmpe})_2\text{Fe}[\text{C},\text{S}-2\text{-Me}(\text{SC}_4\text{H}_3)]$ , the thiophene fragment orbitals are noticeably lower in energy than the fragment metal orbitals.

Although the smaller iron center results in shifts in the metal orbital energies, the same  $\sigma$ -bonding interactions observed in the iridium benzothiophene complex are present. As before, the  $\sigma$  interactions result in the transfer of a pair of electrons from the metal HOMO into bonding metal-ligand orbitals which are primarily localized on the thiophene. The formal oxidation of the metal,  $\text{Fe}^0$  to  $\text{Fe}^{2+}$ , is reflected in a less negative metal charge after insertion ( $-0.54$ ).

Although the primary bonding interactions are similar to those seen in  $\text{Cl}(\text{PMe}_3)_3\text{Ir}[\text{C},\text{S}(\text{SC}_8\text{H}_6)]$ , the HOMO of  $(\text{dmpe})_2\text{Fe}[\text{C},\text{S}-2\text{-Me}(\text{SC}_4\text{H}_3)]$  is different. Recall that for  $\text{Cl}(\text{PMe}_3)_3\text{Ir}[\text{C},\text{S}(\text{SC}_8\text{H}_6)]$  the  $d_{xz}$  orbital interacts with the benzothiophene HOMO to form a

filled bonding/antibonding set of orbitals. The antibonding partner of this set is the HOMO in the complex. For the iron complex, however, the overlap between the metal  $d_{xz}$  orbital and the thiophene HOMO is reduced approximately 25% because of the smaller 3d orbitals of the iron. Because of the reduced overlap and the increased separation in energy between the metal and thiophene orbitals, the thiophene HOMO no longer interacts with the  $d_{xz}$  orbital as it did in the iridium benzothiophene complex. Thus, unlike the iridium complex, the HOMO is now a nonbonding metal orbital instead of an antibonding, ligand-based orbital.

The LUMO of  $(\text{dmpe})_2\text{Fe}[\text{C},\text{S}-2\text{-Me}(\text{SC}_4\text{H}_3)]$  is very similar to Merola's iridium-inserted benzothiophene complex in that the LUMO is predominantly thiophene  $\pi^*$  based (94%) with a large contribution from the  $\alpha$ -carbon. The ligand-based character of the LUMO in both  $\text{Cl}(\text{PMe}_3)_3\text{Ir}[\text{C},\text{S}(\text{SC}_8\text{H}_6)]$  and  $(\text{dmpe})_2\text{Fe}[\text{C},\text{S}-2\text{-Me}(\text{SC}_4\text{H}_3)]$  results from the fact that no metal fragment orbitals interact with the thiophene  $\pi^*$  orbital.

In summary, while the  $\sigma$  bonding and the nature of the LUMO are similar in both  $\text{Cl}(\text{PMe}_3)_3\text{Ir}[\text{C},\text{S}(\text{SC}_8\text{H}_6)]$  and  $(\text{dmpe})_2\text{Fe}[\text{C},\text{S}-2\text{-Me}(\text{SC}_4\text{H}_3)]$ , the filled metal-ligand  $\pi$ - $\pi$  interaction which is a distinguishing feature of the iridium complex (and other 4d and 5d complexes; see below) is absent in the iron complex.

**$\text{Cp}^*(\text{PMe}_3)\text{Rh}[\text{C},\text{S}-2,5\text{-Me}_2(\text{SC}_4\text{H}_2)]$ .** A dimethylthiophene fragment and a  $d^8$   $\text{Cp}^*(\text{PMe}_3)\text{Rh}$  fragment are the basis for the analysis of the bonding interactions in  $\text{Cp}^*(\text{PMe}_3)\text{Rh}[\text{C},\text{S}-2,5\text{-Me}_2(\text{SC}_4\text{H}_2)]$ . The energy level diagrams for the fragments and the molecule are shown in Figure 2. While both ligands on the metal fragment

are electron donors, the moderate donor ability of Cp\* compared to a phosphine ligand is marked, and the resulting charge on the rhodium in the fragment is only  $-0.026$ . This is considerably less negative than the charges on the metals for both the iridium and iron fragments discussed above.

The rhodium-inserted thiophene complex differs from the other complexes described above in that the thiophene ring is bent along the axis formed by the sulfur and the  $\alpha$ -carbon. The bend angle (defined as the angle between the plane formed by S–Rh–C and the least-squares plane formed by all members in the ring of the thiophene, excluding the metal) is  $26^\circ$ .<sup>13</sup> Besides a slight twist, the rest of the thiophene moiety remains fairly flat due to the conjugated  $\pi$  system of the ring. In terms of the interaction diagram, this alteration of structure removes any imposed symmetry restrictions and results in considerable mixing of the thiophene orbitals in the complex. (This mixing is illustrated in the figure by bracketing both the fragment orbitals involved in mixing and bracketing the “mixed” molecular orbitals in the complex. The two brackets are separated by a dashed line. Note: If any orbital in the fragment mixes noticeably with others but also contributes significantly to one particular orbital in the complex, its interaction is still denoted with a solid line.) The general bonding pattern, however, is apparent and is remarkably similar to that of  $\text{Cl}(\text{PMe}_3)_3\text{Ir}[C,S(\text{SC}_8\text{H}_6)]$ .

As expected, the thiophene fragment orbitals are similar in appearance and have energies comparable to the other thiophene fragments already discussed. The SHOMO and LUMO are  $\sigma$  bonding and antibonding orbitals, respectively, and the HOMO is a  $\pi$  orbital with density centered mostly on the sulfur and the  $\alpha$ -carbon. The metal orbitals, however, differ in appearance from those metal fragment orbitals previously discussed. The relative ordering and shapes of the orbitals in the  $\text{Cp}^*(\text{PMe}_3)\text{Rh}$  fragment are dictated by the interactions with Cp\*. Although the metal frontier orbitals of  $\text{Cp}^*(\text{PMe}_3)\text{Rh}$  look different from those of  $\text{Cl}(\text{PMe}_3)_3\text{Ir}$ , the bonding interactions between the metal and thiophene fragments are identical. The metal fragment HOMO and LUMO ( $d_{yz}$  and  $d_{xz}$  orbitals, respectively) combine together in the complex to produce two new orbitals. One of these has electron density directed at the sulfur, and the other has density directed at the  $\alpha$ -carbon. These two orbitals interact with the thiophene SHOMO and LUMO, and these interactions produce the two familiar  $\sigma$  bonds between the thiophene and the metal. The overall result once again is an oxidative addition of rhodium from  $\text{Rh}^+$  to  $\text{Rh}^{3+}$ . A positive increase in metal charge from  $-0.03$  to  $+0.21$  upon insertion reflects the oxidative addition.

While the metal  $d_{xy}$  and  $d_{x^2-y^2}$  orbitals remain non-bonding in the complex, the metal  $d_z$  orbital interacts noticeably with the HOMO of the opened thiophene to form the characteristic high-energy, occupied bonding/antibonding set of orbitals in the complex. (It should not be too surprising that the the metal  $d_z$  orbital interacts with the thiophene HOMO. The angle of the incoming thiophene with respect to the metal is such that the upper portions of the thiophene  $\pi$  lobes overlap with the torus of the  $d_z$  orbital and the lower portions of the thiophene  $\pi$  lobes overlap with the lower lobe of

the  $d_z$  orbital.) The antibonding molecular orbital of the set is the complex's HOMO. As in Merola's iridium benzothiophene complex, the HOMO in  $\text{Cp}^*(\text{PMe}_3)\text{Rh}[C,S-2,5-\text{Me}_2(\text{SC}_4\text{H}_2)]$  has substantial sulfur  $\pi$  character. It is obvious that, regardless of the different metals, ligands, and conformations of the metallacycle, the electronic structures of the two complexes  $\text{Cp}^*(\text{PMe}_3)\text{Rh}[C,S-2,5-\text{Me}_2(\text{SC}_4\text{H}_2)]$  and  $\text{Cl}(\text{PMe}_3)_3\text{Ir}[C,S(\text{SC}_8\text{H}_6)]$  are similar.

One difference between the two complexes, however, is found in the compositions of the lowest energy unoccupied molecular orbital. As already discussed,  $\text{Cl}(\text{PMe}_3)_3\text{Ir}[C,S(\text{SC}_8\text{H}_6)]$  and  $(\text{dmpe})_2\text{Fe}[C,S-2-\text{Me}(\text{SC}_4\text{H}_3)]$  have thiophene-based LUMO's. This is not the case, however, for  $\text{Cp}^*(\text{PMe}_3)\text{Rh}[C,S-2,5-\text{Me}_2(\text{SC}_4\text{H}_2)]$ . The bent geometry of the thiophene ring in  $\text{Cp}^*(\text{PMe}_3)\text{Rh}[C,S-2,5-\text{Me}_2(\text{SC}_4\text{H}_2)]$  and the change in composition of the metal orbitals result in decreased overlap between the metal and thiophene  $\sigma$  orbitals. This has the effect of lowering the energy of the antibonding metal–sulfur  $\sigma$  orbital below the energy of the opened thiophene  $\pi^*$  orbital. Consequently, a metal-based antibonding orbital (with respect to the sulfur) becomes the LUMO of the complex.

**$\text{Cp}^*\text{Ir}(\text{CO})[C,S-2,5-\text{Me}_2(\text{SC}_4\text{H}_2)]$ .** Structurally, this complex and Jones' rhodium-inserted thiophene complex are similar. Both complexes contain the Cp\* ligand and a bent 2,5-Me<sub>2</sub>(SC<sub>4</sub>H<sub>2</sub>) moiety. The donor phosphine ligand in the rhodium complex, however, has been replaced with an acceptor carbonyl ligand. The structural similarities between  $\text{Cp}^*(\text{PMe}_3)\text{Rh}[C,S-2,5-\text{Me}_2(\text{SC}_4\text{H}_2)]$  and  $\text{Cp}^*\text{Ir}(\text{CO})[C,S-2,5-\text{Me}_2(\text{SC}_4\text{H}_2)]$  suggest that the electronic interactions should also be analogous, and this is indeed the case. Since the two complexes are similar, no diagram is shown for the carbonyl species.

Despite the exchange of an acceptor carbonyl for a donor phosphine ligand, the interactions between the metal fragment and the thiophene ligand are identical with those observed in the rhodium complex. Specifically, the formation of two metal–thiophene  $\sigma$  bonds constitutes the oxidative addition of opened thiophene to  $\text{Cp}^*\text{Ir}(\text{CO})$ . Again, a filled metal orbital interacts strongly with the HOMO of the opened thiophene to form an antibonding sulfur-based HOMO in the complex, and the LUMO of the complex is a metal-based, antibonding orbital (with respect to the thiophene sulfur).

**$(\text{PEt}_3)_2\text{Pt}[C,S(\text{SC}_8\text{H}_6)]$ .** The calculated energy level diagrams for  $(\text{PEt}_3)_2\text{Pt}[C,S-S(\text{C}_8\text{H}_6)]$  and for the  $(\text{PEt}_3)_2\text{Pt}$  and benzothiophene fragments are shown in Figure 3. The d<sup>8</sup> platinum-inserted benzothiophene complex is essentially square planar (despite a slight umbrella effect and L–M–L bond angle distortions),<sup>5</sup> with the benzothiophene occupying two adjacent coordination sites and the donor phosphine ligands occupying the other two coordination sites.

The  $C_{2v}$  symmetry of the d<sup>10</sup>  $(\text{PEt}_3)_2\text{Pt}$  fragment is apparent in the structure and arrangement of the metal orbitals. The most notable effects of the  $C_{2v}$  symmetry on the metal orbitals are the appearance of the low-lying  $a_1$  and  $p_z$  orbitals. The metal  $a_1$  orbital which is derived from the metal–ligand, antibonding  $\sigma$  orbital ( $a_{1g}$ ) present in a  $D_{4h}$  ML<sub>4</sub> molecule<sup>29</sup> is stabilized by the loss of two ligands, whereas the  $p_z$  orbital is stabilized by

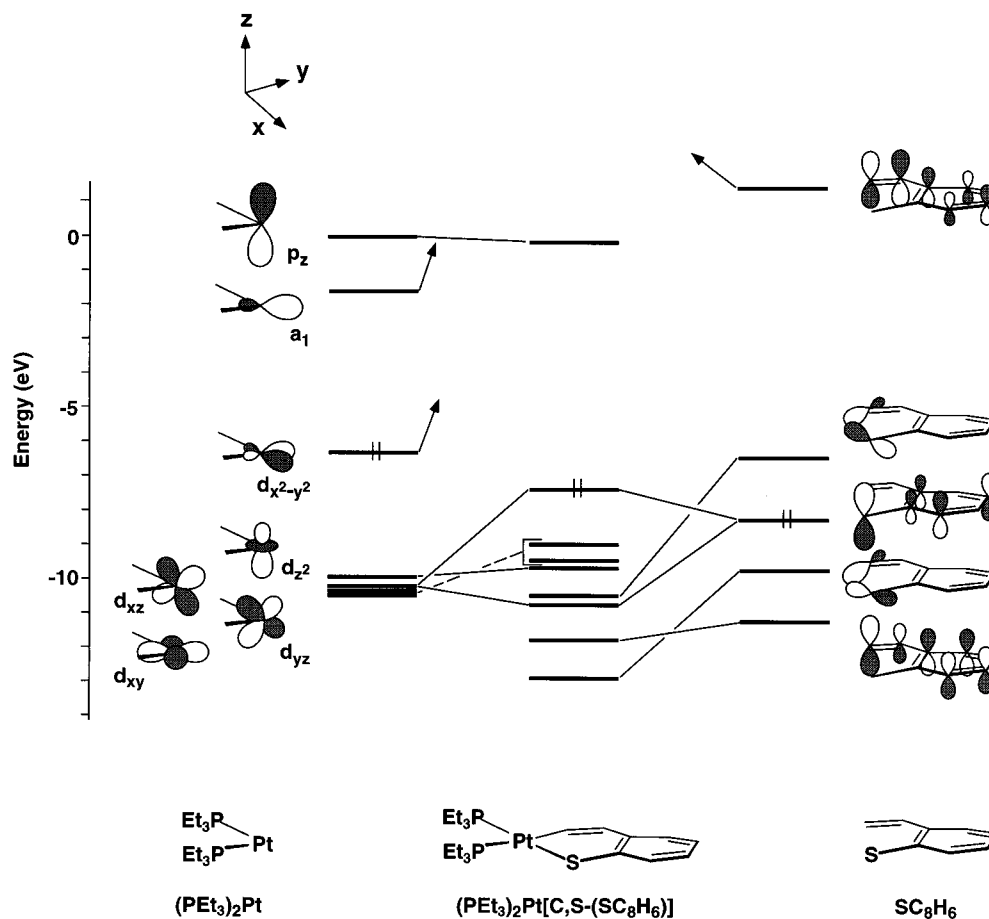


**Figure 3.** Calculated energy level diagrams for  $(\text{PEt}_3)_2\text{Pt}[C,S-(\text{SC}_8\text{H}_6)]$  and for the  $(\text{PEt}_3)_2\text{Pt}$  and the opened benzothiophene fragments.

the absence of ligands along the  $z$  axis. The  $d_{x^2-y^2}$  orbital is also stabilized to some degree from the loss of one half of the antibonding interactions present in an  $\text{ML}_4$  environment. In the  $\sigma$ -donor environment of the platinum fragment, the  $d_{xy}$ ,  $d_{xz}$ , and  $d_{yz}$  orbitals are degenerate and are nonbonding with respect to the phosphine ligands. The  $d_{z^2}$  orbital, on the other hand, is slightly destabilized because it is antibonding with respect to the triethylphosphine groups. The opened benzothiophene molecular orbitals are similar in energy and appearance to those for the other complexes.

Like Merola's iridium benzothiophene complex, the metal orbitals involved in bonding with the opened benzothiophene are  $\sigma$  orbitals formed from mixing two metal orbitals. The  $a_1$  and the  $d_{x^2-y^2}$  metal fragment orbitals mix together upon complex formation to form one orbital directed at the incoming sulfur and one directed at the  $\alpha$ -carbon. Bond formation thus results from the donation of electron density from the metal HOMO and benzothiophene SHOMO into the benzothiophene LUMO and the metal LUMO, respectively. A net transfer of a pair of electrons from the metal to the benzothiophene occurs and is once again reflected in a more positive charge on the metal after insertion. The metal charge increases from  $-0.79$  to  $-0.38$  after insertion.

Once again, the HOMO of the complex is an antibonding orbital resulting from interactions between the opened benzothiophene HOMO, a  $\pi$  orbital with large

sulfur contribution, and the filled metal  $d_{xz}$ . The character of the complex's HOMO is, as expected, predominantly sulfur. The LUMO, on the other hand, is essentially the metal  $p_z$  orbital. Although a metal-based LUMO is not uncommon for these complexes, the fact that this molecular orbital is not directed at a ligand, a consequence of the coordinatively unsaturated nature of the complex, is unique. It is worthwhile at this point to reemphasize the reactivity of this complex toward hydridic reagents. Because of the accessibility and character of the LUMO of the complex, it is not unreasonable to think of the metal as the nucleophilic attack site.

**(triphos)Ir[C,S-(SC<sub>8</sub>H<sub>6</sub>)]<sup>+</sup>.** The energy level diagrams for the complex and for the [(triphos)Ir]<sup>+</sup> and the opened benzothiophene fragments are shown in Figure 4. The (triphos)Ir[C,S-(SC<sub>8</sub>H<sub>6</sub>)]<sup>+</sup> cation represents the second example of a five-coordinate, transition-metal-inserted thiophene complex. (The first example was Angelici's  $\text{Cp}^*\text{Ir}[C,S-2,5-\text{Me}_2(\text{SC}_4\text{H}_2)]$ . The electronic structure of this molecule was discussed in detail in a previous paper.)<sup>30</sup> The unique coordination geometry of Bianchini's molecule is achieved through coordination of a tridentate phosphorus ligand. The molecular orbitals for this  $C_{3v}$   $\text{ML}_3$  fragment are derived from those of an octahedron except for a change in composition. In terms of a coordinate system which places the  $z$  axis coincident with the 3-fold axis of the  $\text{ML}_3$  fragment, the  $t_{2g}$  set ( $1a_1$ ,  $1e_s$ , and  $1e_a$ ) becomes primarily  $z^2$ ,  $x^2 - y^2$ , and  $xy$ ; however,  $yz$  and  $xz$  mix with

(29) Albright, T. A.; Burdett, J. K.; Whangbo, M. H. *Orbital Interactions in Chemistry*; Wiley: New York, 1985.

(30) Harris, S. *Organometallics* **1994**, *13*, 2628.

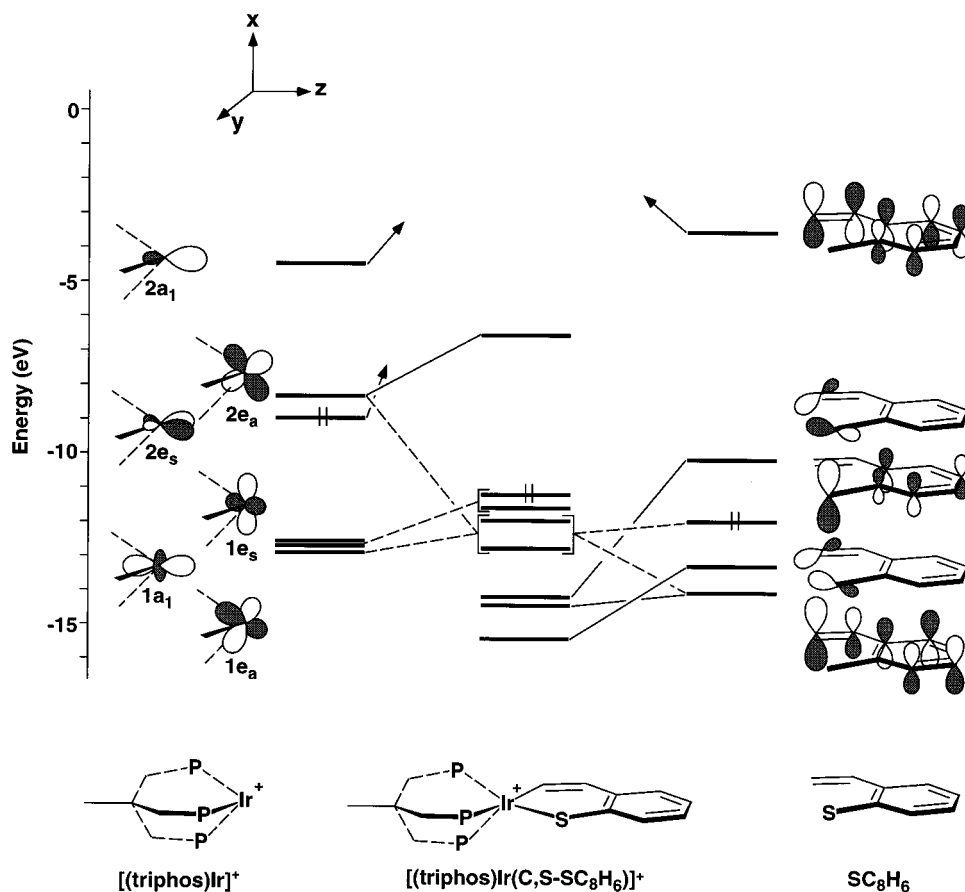


**Figure 4.** Calculated energy level diagrams for  $(\text{triphos})\text{Ir}[\text{C},\text{S}-(\text{SC}_8\text{H}_6)]^+$  and for the  $[(\text{triphos})\text{Ir}]^+$  and the opened benzothiophene fragments.

$x^2 - y^2$  and  $xy$ , respectively, so that the orbitals lie between the M–L bonds. Also, the  $e_g$  set ( $2e_s$  and  $2e_a$ ) becomes primarily  $yz$  and  $xz$ , but slight mixing of the  $e_g$  set with  $x^2 - y^2$  and  $xy$  results in orbitals that are directed at the three phosphine ligands. Also, the  $\text{ML}_3$   $e_g$  set is stabilized compared to the  $e_g$  set of an octahedron due to a loss of half of the antibonding interactions of the metal with ligand lone pair orbitals.<sup>29</sup> Finally, the loss of three ligands produces a low-lying  $\sigma$  ( $2a_1$ ) orbital. Overall, the  $C_{3v}$  symmetry of the metal fragment produces a distinctive set of fragment orbitals when compared to other metal-inserted complexes. Most importantly, the metal fragment LUMO for this complex is a  $\pi$  orbital with respect to the benzothiophene rather than the expected  $\sigma$  orbital and, consequently, plays a much different role in the bonding of the complex.

The uniqueness of the metal orbitals is evident in the interactions of the metal with the benzothiophene fragment. Because of the  $C_{3v}$  symmetry of the metal fragment, four metal orbitals ( $1a_1$ ,  $1e_s$ ,  $2e_s$ , and  $2a_1$ ) participate in  $\sigma$ -bonding interactions with the two benzothiophene  $\sigma$  orbitals (SHOMO and LUMO). Combinations of these four metal orbitals with combinations of the two benzothiophene orbitals form two  $\sigma$  bonding orbitals, two  $\sigma$  nonbonding orbitals, and two  $\sigma$  antibonding orbitals. The strongest of the bonding interactions is between a metal orbital composed of  $2e_s$  and  $1a_1$  and a benzothiophene orbital composed of the SHOMO and LUMO. Both the metal and ligand orbital combinations produce electron density localized between the metal and the sulfur, and this concentration of density produces strong overlap between the iridium and the sulfur.

The second  $\sigma$ -bonding interaction, considerably weaker than the first, results from a mixture of metal orbitals which directs electron density at both the sulfur and  $\alpha$ -carbon interacting with the benzothiophene LUMO. The two nonbonding  $\sigma$  orbitals, which are primarily metal-based, form the HOMO and the SHOMO of the complex. The two  $\sigma$  antibonding orbitals lie high in energy and are unoccupied. Overall, the metal–ligand  $\sigma$  orbital interactions in this molecule differ from those seen in the other complexes, where only the HOMO and LUMO of the metal fragment participate in  $\sigma$  bond formation.

The  $\pi$  orbital interactions for this complex are also unique. In the other complexes, the important  $\pi$  interaction is between the thiophene HOMO and a filled “ $\pi$ ” metal orbital. The product is a bonding/antibonding pair of orbitals; the antibonding partner is the HOMO of the complex. The only filled metal “ $\pi$ ” orbital in the  $[(\text{triphos})\text{Ir}]^+$  fragment ( $1e_a$ ), however, is not oriented properly to interact with the benzothiophene HOMO. Instead, the empty metal  $2e_a$  “ $\pi$ ” orbital interacts with the sulfur electron density of the benzothiophene HOMO. This leads to a weakly bonding molecular orbital and an antibonding counterpart. This antibonding orbital forms the LUMO of the complex (not the HOMO as in the other complexes). The relatively large separation in energy between the metal  $2e_a$  orbital and the benzothiophene HOMO, however, results in the LUMO of the complex being almost entirely metal in character. Like the square-planar platinum-inserted compound,  $(\text{triphos})\text{Ir}[\text{C},\text{S}-(\text{SC}_8\text{H}_6)]^+$  has both a metal-based LUMO and a coordination site open to nucleophilic attack (this coordination site is somewhat hindered due to the bulky



triphos ligand). The reported reactivity of this complex does include hydride attack at the metal.<sup>6,7</sup>

It should be evident from the bonding description that a considerable amount of the total electron density between the metal and benzothiophene is localized between the iridium and the sulfur. In the other complexes, a more equal distribution of density between the metal center and the sulfur and  $\alpha$ -carbon atoms is observed. Also, additional metal–sulfur  $\pi$  bonding is seen for (triphos)Ir[*C,S*-(SC<sub>8</sub>H<sub>6</sub>)]<sup>+</sup> which is not observed for the other complexes. The  $\pi$  bonding between the metal and the thiophene HOMO is canceled in all other complexes by a filled antibonding partner. For the (triphos)Ir complex, however, the  $\pi$  antibonding molecular orbital is unoccupied and, therefore, the result is a net bonding interaction. The increased M–S density and the additional M–S  $\pi$  bonding are consistent with the fact that (triphos)Ir[*C,S*-(SC<sub>8</sub>H<sub>6</sub>)]<sup>+</sup> has the shortest M–S and the longest M–C bonds for any of the metal-inserted complexes.

As in the other complexes, the insertion of iridium into the C–S bond of the benzothiophene can be viewed as an oxidative addition. The calculated charge on the Ir(I) in the [(triphos)Ir]<sup>+</sup> fragment is –0.64. Formally oxidizing the metal to Ir(III), however, has little effect on the metal charge; the charge on the metal after insertion is –0.54. Oxidation of the metals in the other complexes results in significant changes in metal charge. In this respect, (triphos)Ir[*C,S*-(SC<sub>8</sub>H<sub>6</sub>)]<sup>+</sup> is similar to Angelici's Cp\*Ir[*C,S*-2,5-Me<sub>2</sub>(SC<sub>4</sub>H<sub>2</sub>)] in that participation of the metal orbitals in the  $\pi$  system of the benzothiophene forces electron density back onto the metal. The orbital structures of both complexes show evidence of this delocalization, since the third and fourth highest energy occupied molecular orbitals consist of similar amounts of metal and ligand  $\pi$  character. The  $\pi$  delocalization in these complexes is reflected in equivalent C–C bond distances.

**Metallacycle Geometries.** Much discussion in the literature has centered around the significance of the fact that some metallathiacycles have bent geometries while others have planar geometries. The complexes which contain bent metallacycles all exhibit a localized diene-like structure. The localized structure is generally characterized by shorter M–C bonds, longer M–S and S–C bonds, and an alternation of long and short C–C bond distances. The upfield <sup>1</sup>H resonances also give a reasonable indication of the localized diene structure. The planar metallacycles exhibit both localized and delocalized structures. Delocalization in the structures is best identified, in addition to more equivalent C–C bond distances, by downfield <sup>1</sup>H chemical shifts.<sup>5,7,31</sup>

A number of explanations for the different ring conformations have been put forth. In 16e<sup>–</sup> complexes such as Cp\*Ir[*C,S*-2,5-Me<sub>2</sub>(SC<sub>4</sub>H<sub>2</sub>)], metallacycle planarity serves to stabilize these complexes by allowing for the delocalization of  $\pi$  electron density from the ring atoms back onto the metal. Metallacycle bending, which is observed exclusively in 18e<sup>–</sup> complexes, could prevent unnecessary metal–ligand  $\pi$  delocalization. It then becomes a question as to why Merola's Cl(PMe<sub>3</sub>)<sub>3</sub>Ir[*C,S*-(SC<sub>8</sub>H<sub>6</sub>)], Field's (dmpe)<sub>2</sub>Fe[*C,S*-2-Me<sub>2</sub>(SC<sub>4</sub>H<sub>3</sub>)], and Mait-

lis's (PEt<sub>3</sub>)<sub>2</sub>Pt[*C,S*-(SC<sub>8</sub>H<sub>6</sub>)] have not only localized bonding structures but also planar metallacycles. Merola attributes the planarity of the metallacycle in his system to steric congestion caused by the flanking trimethylphosphine groups.<sup>11</sup> The ring system does indeed rest in a steric pocket, as demonstrated through space-filling models. It should not be difficult, on the basis of the similarities in ligands and coordination environments, to extend this rationalization to Field's complex. Maitlis's square-planar, platinum complex, on the other hand, contains a planar metallacycle but is not sterically forced into such a configuration. On the basis of this observation, it is difficult to determine whether the ring systems in Merola's and Field's complexes are forced into planarity by a restrictive environment or if planarity is inherently favorable.

One possible electronic explanation for a bent-metallacycle geometry stems from the antibonding nature of the HOMO in these complexes. For example, although the HOMO in Cp\*(PMe<sub>3</sub>)Rh[*C,S*-2,5-Me<sub>2</sub>(SC<sub>4</sub>H<sub>2</sub>)] is antibonding between the metal and the opened thiophene fragment, bending may alleviate, to some extent, this unfavorable interaction. Bending the metallacycle reorients the sulfur electron lone pairs and may effectively reduce some of the antibonding nature of the HOMO. (This characteristic of sulfur to attain specific geometries in order to isolate a pair of electrons from bonding interactions is nicely illustrated in the known S-bound thiophene complexes in which the thiophene bonds to the metal at an angle so that only one pair of electrons on the sulfur interacts with the metal.)<sup>30</sup> To determine if bending does reduce the antibonding character of the HOMO, molecular orbital calculations were performed on planar isomers of the complexes which contain bent metallacycles. That is, the rings in these bent systems were artificially flattened, and the calculations for the planar isomers were compared to the calculations on the original, known structures. The results of these calculations indicate no electronic preference for planar or bent metallacycles; the antibonding character of the HOMO is not reduced upon bending of the ring, and the orbital structures for the planar and bent isomers of a particular complex are virtually indistinguishable.

Since no electronic preferences are apparent for either bent or planar metallacycles and since this explanation cannot account for the planarity of the benzothiophene in (PEt<sub>3</sub>)<sub>2</sub>Pt[*C,S*-(SC<sub>8</sub>H<sub>6</sub>)], which also has an antibonding HOMO, molecular mechanics calculations were employed to determine how steric factors might influence ring geometries. The results of these calculations for complexes which exhibit bent ring geometries showed that in general it is possible to identify sterically hindering groups which force the ring system into the bent conformation. To illustrate, molecular mechanics calculations on Cp\*(PMe<sub>3</sub>)Rh[*C,S*-2,5-Me<sub>2</sub>(SC<sub>4</sub>H<sub>2</sub>)] predict a flattening of the ring system when sterically bulky groups are reduced in size. For example, replacing Cp\* with Cp results in a flatter metallacycle upon minimization. (Other groups on this complex which also influence the ring geometry are discussed in another paper.)<sup>32</sup> The combined results of the molecular orbital and molecular mechanics calculations thus indicate that

(31) Chen, J.; Daniels, L. M.; Angelici, R. J. *J. Am. Chem. Soc.* **1990**, *112*, 199.

(32) Blonski, C.; Myers, A. W.; Palmer, M.; Harris, S.; Jones, W. D. Submitted for publication in *Organometallics*.

bending is a steric rather than electronic effect and that planar metallacycle rings occur in complexes such as  $\text{Cl}(\text{PMe}_3)_3\text{Ir}[C,S-(\text{SC}_8\text{H}_6)]$ ,  $(\text{dmpe})_2\text{Fe}[C,S-2\text{-Me}_2(\text{SC}_4\text{H}_3)]$ , and  $(\text{PEt}_3)_2\text{Pt}[C,S-(\text{SC}_8\text{H}_6)]$  because no ligands are present to force the ring systems to bend.

The two complexes having a delocalized metallathia-benzene structure, Angelici's  $\text{Cp}^*\text{Ir}[C,S-2,5\text{-Me}_2(\text{SC}_4\text{H}_2)]$  and Bianchini's  $(\text{triphos})\text{Ir}[C,S-(\text{SC}_8\text{H}_6)]^+$ , are formally  $16e^-$  complexes. Although the ancillary ligands are not identical ( $\text{Cp}^*$  and triphos), both metal-inserted complexes contain a  $\text{ML}_3$  metal fragment, and consequently, their orbital structures are remarkably similar. The significance of the  $\text{ML}_3$  fragment is the presence of an empty metal " $\pi$ " orbital which can accept electron density from the thiophene  $\pi$  system. In Angelici's complex, the delocalization of electronic charge from the ring atoms onto the metal serves to stabilize the complex, which, under other circumstances, would be electron-deficient. The stability of  $(\text{triphos})\text{Ir}[C,S-(\text{SC}_8\text{H}_6)]^+$ , despite the much more negatively charged metal center, is also achieved through back-donation from the thiophene  $\pi$  system. The delocalization in Angelici's and Bianchini's complexes appears to be a consequence of both the electron deficiency of the molecules and the  $\pi$ -acceptor ability of the  $\text{ML}_3$  LUMO that is characteristic of these  $16e^-$  complexes. Clearly, these factors are heavily dependent on each other. Localized structures are observed in Merola's, Field's, and Maitlis's planar metallacycle complexes not only because the molecules are  $18e^-$  complexes (or, for the Pt complex, a stable  $16e^-$  square-planar complex) but also because these complexes do not have empty metal " $\pi$ " orbitals available for donation from the thiophene. The significance of electron deficiency and the associated empty  $\pi$  orbital of the  $\text{ML}_3$  fragment in relation to ring delocalization is apparent, because hydride addition to  $(\text{triphos})\text{Ir}[C,S-(\text{SC}_8\text{H}_6)]^+$  and other analogous complexes leads to complexes having localized C–C bonds.<sup>7,8</sup> This localization can be attributed to the new  $18e^-$  configuration and the corresponding loss of the metal  $\pi$  orbital responsible for delocalization.

**Reactivity.** Reports of reactivity for the transition-metal-inserted thiophene complexes are scarce. Of those discussed here, only the platinum and the  $(\text{triphos})\text{Ir}$  complexes have demonstrated an ability to remove sulfur from thiophenic molecules. On the basis of the calculated electronic structure for the benzothiophene analog, protonation of the platinum dibenzothiophene complex (eq 3) to produce 2-phenylthiophenol<sup>4</sup> appears to occur via initial attack at the thiophenic sulfur. That is, electrophilic attack at the sulfur is expected due to the high-energy, sulfur-based HOMO of the complex and the negatively charged sulfur atom. (Calculations on both metal-inserted thiophene and benzothiophene complexes and preliminary calculations on several dibenzothiophene complexes suggest that the particular thiophenic moiety present in a complex does not significantly affect the bonding between the thiophenic ligand and a particular metal fragment. Bonding interactions are nearly identical, for example, in  $\text{Cp}^*(\text{PMe}_3)\text{Rh}(\text{T})$ ,  $\text{Cp}^*(\text{PMe}_3)\text{Rh}(\text{BT})$ , and  $\text{Cp}^*(\text{PMe}_3)\text{Rh}(\text{DBT})$  complexes.) On the basis of their similar electronic structures, a number of the other complexes discussed should be susceptible to electrophilic attack at sulfur. In particular,  $\text{Cl}(\text{PMe}_3)_3\text{Ir}[C,S-$

**Table 1. Percentage of Metal and Sulfur Character of the HOMO**

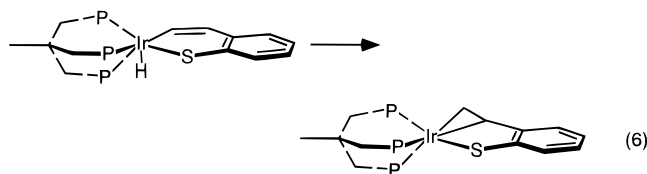
	metal	sulfur
$\text{Cl}(\text{PMe}_3)_3\text{Ir}[C,S-(\text{SC}_8\text{H}_6)]$	25	50
$(\text{dmpe})_2\text{Fe}[C,S-2\text{-Me}(\text{SC}_4\text{H}_3)]$	97	1
$\text{Cp}^*(\text{PMe}_3)\text{Rh}[C,S-2,5\text{-Me}_2(\text{SC}_4\text{H}_2)]$	27	33
$\text{Cp}^*(\text{CO})\text{Ir}[C,S-2,5\text{-Me}_2(\text{SC}_4\text{H}_2)]$	32	36
$(\text{PEt}_3)_2\text{Pt}[C,S-(\text{SC}_8\text{H}_6)]$	19	49
$(\text{triphos})\text{Ir}[C,S-(\text{SC}_8\text{H}_6)]^+$	80	18

$(\text{SC}_8\text{H}_6)]$ ,  $\text{Cp}^*(\text{PMe}_3)\text{Rh}[C,S-2,5\text{-Me}_2(\text{SC}_4\text{H}_2)]$ , and  $\text{Cp}^*\text{Ir}(\text{CO})[C,S-2,5\text{-Me}_2(\text{SC}_4\text{H}_2)]$  have sulfur-based HOMO's similar to that in  $(\text{PEt}_3)_2\text{Pt}[C,S-(\text{SC}_8\text{H}_6)]$  (Table 1), and the sulfur in these complexes should also be nucleophilic. Additional evidence to support reactivity at the sulfur in saturated complexes has been provided by Bianchini and co-workers. They have demonstrated selective attack of  $\text{Me}^+$  and  $\text{H}^+$  at sulfur for the 18-electron hydride species  $(\text{triphos})\text{Ir}(\text{H})[C,S-(\text{SC}_8\text{H}_6)]$  and its thiophene and dibenzothiophene analogs.<sup>33</sup> Although no molecular orbital structure has been calculated for these  $(\text{triphos})\text{Ir}$  hydride complexes (no X-ray structures exist), similarities in ligands and coordination geometries suggest that both the molecular and electronic structures of  $(\text{triphos})\text{Ir}(\text{H})[C,S-(\text{SC}_8\text{H}_6)]$  and its analogs should be quite similar to those of the other  $d^6$  octahedral complexes discussed (e.g.  $\text{Cl}(\text{PMe}_3)_3\text{Ir}[C,S-(\text{SC}_8\text{H}_6)]$ ). That is, the HOMO in these hydride complexes is expected to be an antibonding, sulfur-based orbital.

The orbital structures of the  $16e^-$  complexes  $(\text{triphos})\text{Ir}[C,S-(\text{SC}_8\text{H}_6)]^+$  and  $\text{Cp}^*\text{Ir}[C,S-2,5\text{-Me}_2(\text{SC}_4\text{H}_2)]$  suggest that the sulfur center in these complexes should not be susceptible to electrophilic attack. The sulfur  $\pi$  orbital which is localized in the HOMO of the  $18e^-$  complexes is now involved in delocalized metal–ligand bonding. This difference in orbital character is consistent with the fact that  $\text{H}^+$  does not attack the sulfur atom in  $(\text{triphos})\text{Ir}[C,S-(\text{SC}_8\text{H}_6)]^+$  but does attack the sulfur atom in the 18-electron hydride species  $(\text{triphos})\text{Ir}(\text{H})[C,S-(\text{SC}_8\text{H}_6)]$  (see above).

Hydridic attack on  $(\text{PEt}_3)_2\text{Pt}[C,S-(\text{SC}_8\text{H}_6)]$  has been suggested to occur via initial H–X oxidative addition to the metal.<sup>5</sup> Because the LUMO of the complex is metal-based, low in energy, and easily accessible due to its perpendicular orientation to the plane of the molecule, attack in this fashion is not unexpected. The hydridic attack on  $(\text{triphos})\text{Ir}[C,S-(\text{SC}_8\text{H}_6)]^+$  to produce a metal–hydride species appears to be promoted by different factors. Although the LUMO is primarily metal in character, the bulky triphos ligand limits, to a large extent, the accessibility of this orbital. Attack at iridium by a hydride, therefore, may be driven by the electron-deficient nature of the complex. While the metal–hydride species is only a kinetic product of this reaction, it may serve as a temporary stabilization factor for the complex. Thermodynamically, the hydride selectively rearranges to the  $\alpha$ -carbon to produce an  $\eta^3$  complex (eq 6).<sup>7</sup> This migration may be a direct consequence of the steric bulk of the triphos ligand. Rearrangement of the hydride to the  $\alpha$ -carbon leaves the molecule less crowded sterically but retains a stable  $18e^-$  configuration. This behavior, thermal rearrange-

(33) Bianchini, C.; Casares, J. A.; Jimenez, M. V.; Meli, A.; Moneti, S.; Vizza, F.; Herrera, V.; Sánchez-Delgado, R. *Organometallics* **1995**, *14*, 4850.



ment of a metal-hydride to the  $\alpha$ -carbon, has been observed in other metal-inserted thiophene complexes containing the triphos ligand.<sup>8,27,34</sup> It is not so surprising that the migration is selective toward the  $\alpha$ -carbon, given the low calculated charge on the  $\alpha$ -carbon ( $-0.040$ ) and the fact that migration to the sulfur would probably result once again in a  $16e^-$  complex.

Hydride rearrangement has not been observed for  $(\text{PEt}_3)_2\text{Pt}[C,S-(\text{SC}_8\text{H}_6)]$ , possibly because of the lack of bulky ligands such as triphos and the fact that the  $\alpha$ -carbon charge for this complex is much more negative ( $-0.29$  compared to  $-0.040$  for the  $\alpha$ -carbon in  $(\text{triphos})\text{Ir}[C,S-(\text{SC}_8\text{H}_6)]^+$ ). Hydride migration to the  $\alpha$ -carbon has also not been observed in  $\text{Cp}^*\text{Ir}(\text{H}_2)[C,S-2,5-\text{Me}_2(\text{SC}_4\text{H}_2)]^{14}$  (the dihydride analog to the carbonyl complex). Three conditions most likely contribute to the stability of the metal-bound hydrides of this system: the relatively positive metal center, the negatively charged  $\alpha$ -carbon, and the lack of a bulky ligand to induce migration. Finally, although the LUMO's of some of the other complexes are also metal-based, nucleophilic attack at the metal in these complexes is hindered by both crowded ligand spheres and the saturated nature of the compounds.

Both the platinum- and the  $(\text{triphos})\text{Ir}$ -inserted complexes exhibit two other interesting features. First, both complexes maintain relatively high negative charges on the metal despite the oxidative addition of the thiophene moieties. Overall, trends observed in metal charges correlate with the number of donor ligands bound to the metal; i.e. a greater number of donor ligands results in a more negatively charged metal center (Table 2). (This trend holds both before and after metal insertion.) The ultimate reactivity of these complexes may be somewhat regulated by the metal charge, since two of the complexes with high negative charges are indeed reactive. Second, both  $(\text{PEt}_3)_2\text{Pt}[C,S-(\text{SC}_8\text{H}_6)]$  and  $(\text{triphos})\text{Ir}[C,S-(\text{SC}_8\text{H}_6)]^+$  exhibit the strongest M-S and M-C bonds as determined by calculated bond orders (Table 3). This is interesting in that the strengths of the bonds from the thiophene to the metal do not appear to significantly influence the ability of the M-S and M-C bonds to be cleaved.

The effect of ring geometries on the reactivities of the complexes is not clear. Although the two complexes that show reactivities toward sulfur removal,  $(\text{PEt}_3)_2\text{Pt}[C,S-(\text{SC}_8\text{H}_6)]$  and  $(\text{triphos})\text{Ir}[C,S-(\text{SC}_8\text{H}_6)]^+$ , contain planar metallacycles, they have different metallacycle bonding structures, localized and delocalized, respectively. This makes it apparent that delocalization, or the lack thereof, cannot be directly correlated with reactivity. Furthermore, similarities in the orbital structures of saturated complexes containing both bent and planar metallacycles suggest that the geometry of the ring

**Table 2. Calculated Charge on the Metal both before and after Insertion into the Thiophene Moiety<sup>a</sup>**

	before	after
$(\text{dmpe})_2\text{Fe}[C,S-2-\text{Me}(\text{SC}_4\text{H}_3)]$	-1.109	-0.540
$(\text{triphos})\text{Ir}[C,S-(\text{SC}_8\text{H}_6)]^+$	-0.644	-0.542
$\text{Cl}(\text{PMe}_3)_3\text{Ir}[C,S-(\text{SC}_8\text{H}_6)]$	-0.841	-0.476
$(\text{PEt}_3)_2\text{Pt}[C,S-(\text{SC}_8\text{H}_6)]$	-0.785	-0.377
$\text{Cp}^*(\text{PMe}_3)\text{Rh}[C,S-2,5-\text{Me}_2(\text{SC}_4\text{H}_2)]$	-0.026	0.209
$\text{Cp}^*(\text{CO})\text{Ir}[C,S-2,5-\text{Me}_2(\text{SC}_4\text{H}_2)]$	0.590	0.782

<sup>a</sup> The complexes are arranged according to the number of donor ligands they contain.

**Table 3. Calculated M-S and M-C Bond Orders**

	M-S	M-C
$\text{Cl}(\text{PMe}_3)_3\text{Ir}[C,S-(\text{SC}_8\text{H}_6)]$	0.718	0.860
$(\text{dmpe})_2\text{Fe}[C,S-2-\text{Me}(\text{SC}_4\text{H}_3)]$	0.456	0.729
$\text{Cp}^*(\text{PMe}_3)\text{Rh}[C,S-2,5-\text{Me}_2(\text{SC}_4\text{H}_2)]$	0.660	0.785
$\text{Cp}^*(\text{CO})\text{Ir}[C,S-2,5-\text{Me}_2(\text{SC}_4\text{H}_2)]$	0.704	0.783
$(\text{PEt}_3)_2\text{Pt}[C,S-(\text{SC}_8\text{H}_6)]$	0.779	0.877
$(\text{triphos})\text{Ir}[C,S-(\text{SC}_8\text{H}_6)]^+$	1.116	0.905

system in these complexes is not important in terms of desulfurization chemistry.

## Conclusions

Results of Fenske-Hall molecular orbital calculations show that a number of transition-metal-inserted thiophene complexes have similar electronic structures. These similarities exist despite differences in metals, ligands, coordination geometries, and metallacycle geometries. All of the complexes can be viewed as forming via an oxidative addition of an opened thiophene to a transition metal, which results in the formation of M-S and M-C  $\sigma$  bonds. The oxidative addition of the thiophene moiety is evidenced both in the transfer of a pair of metal electrons into a metal-thiophene bonding orbital which is primarily localized on the ligand and by the more positive metal charges after metal insertion into the C-S bond.

Differences in metal centers have fairly predictable effects on the orbital structures of the complexes. The metal-thiophene interactions in the Rh, Ir(CO), and Pt complexes are similar. Differences in the electronic structure of the Fe complex result from the high negative charge on the metal and the small size of the metal. While the HOMO in the Rh, Ir(CO), and Pt complexes is a sulfur-based antibonding  $\pi$  orbital, the HOMO in the Fe complex is a metal-based nonbonding orbital. The large sulfur character of the HOMO seen in many of the complexes is consistent with the fact that the sulfur in both  $(\text{PEt}_3)_2\text{Pt}[C,S-(\text{SC}_8\text{H}_6)]$  and  $(\text{triphos})\text{Ir}(\text{H})[C,S-(\text{SC}_8\text{H}_6)]$  is reactive toward electrophiles. Similarities in the orbital structures of a number of the complexes suggest that they may also be susceptible to such attack. The  $16e^-$  complex  $(\text{triphos})\text{Ir}[C,S-(\text{SC}_8\text{H}_6)]^+$  is not expected to be reactive at the sulfur, since in this complex the sulfur  $\pi$  orbital is involved in delocalized metal-ligand bonding. The sulfur in the  $(\text{triphos})\text{Ir}$  complex only becomes electrophilic upon formation of the  $18e^-$  hydride species, whose electronic structure is predicted to be analogous to the other  $18e^-$  complexes discussed in this paper.

The effect of the different ligands on the bonding in the complexes is associated with the ligand donor ability. The number of donor ligands and their ability to donate electron density to the metal correlate pre-

(34) Bianchini, C.; Frediani, P.; Herrera, V.; Jimenez, M. V.; Meli, A.; Rincon, L.; Sánchez-Delgado, R.; Vizza, F. *J. Am. Chem. Soc.* **1995**, *117*, 4333.

cisely with the charge on the metal. The charge on the metal, generally calculated to be quite negative, may play some part in the reactivity of the complexes. Both the platinum and the (triphos)Ir complexes, which are C–S bond activated, have relatively high negative charges even after the oxidative addition of the thiophene.

The reactivity of  $(\text{PEt}_3)_2\text{Pt}[C,S(\text{SC}_8\text{H}_6)]$  and (triphos)Ir $[C,S(\text{SC}_8\text{H}_6)]^+$  with hydride reagents can be related to their orbital structures and geometries; that is, both have low-energy, metal-based LUMO's and an open coordination site. While  $\text{Cp}^*(\text{PMe}_3)\text{Rh}[C,S-2,5\text{-Me}_2(\text{SC}_4\text{H}_2)]$  and  $\text{Cp}^*\text{Ir}(\text{CO})[C,S-2,5\text{-Me}_2(\text{SC}_4\text{H}_2)]$  also have metal-based LUMO's, they are coordinatively saturated and therefore do not have a low-lying, accessible, empty metal orbital. Both  $\text{Cl}(\text{PMe}_3)_3\text{Ir}[C,S(\text{SC}_8\text{H}_6)]$  and  $(\text{dmpe})_2\text{Fe}[C,S-2\text{-Me}_2(\text{SC}_4\text{H}_3)]$ , on the other hand, have ligand-based LUMO's.

The delocalization observed in the metallacycle of (triphos)Ir $[C,S(\text{SC}_8\text{H}_6)]^+$  and other  $16e^-$  complexes is attributed to the electron deficiency of these complexes and the characteristic orbital structure of the  $\text{ML}_3$  fragment associated with these molecules. Such a fragment produces an empty metal  $\pi$  orbital which is able to accept electron density from the thiophene ring system. The resultant delocalization serves to stabilize

these electron-deficient complexes. Since all the other molecules discussed have stable electron configurations and, correspondingly, do not contain empty metal  $\pi$  orbitals, complexes such as  $\text{Cl}(\text{PMe}_3)_3\text{Ir}[C,S(\text{SC}_8\text{H}_6)]$  and  $(\text{PEt}_3)_2\text{Pt}[C,S(\text{SC}_8\text{H}_6)]$  have localized metallacycle structures.

Molecular orbital calculations performed on planar and bent isomers of  $\text{Cp}^*(\text{PMe}_3)\text{Rh}[C,S-2,5\text{-Me}_2(\text{SC}_4\text{H}_2)]$  suggest that electronic factors are not significant in determining whether the metallacycle will adopt a bent or planar geometry. Steric factors, determined through molecular mechanics calculations, appear to define the preferred metallacycle conformation. In addition, the similar orbital structures of complexes with bent and planar ligands suggest that metallacycle geometry will not affect bond activation reactivities. Both the molecular orbital and molecular mechanics calculations employed to determine the sources of particular ring geometries will be discussed more thoroughly in another paper.<sup>32</sup>

**Acknowledgment.** Financial support of this research by the National Science Foundation (Grant CHE94-21784) is greatly appreciated. M.P. also thanks the NSF EPSCoR and DOE EPSCoR for support.

OM960707N